Available online at www.sciencedirect.com
ScienceDirect
Nuclear Medicine and Biology xx (2010) xxx – xxx
NUCLEAR MEDICINE — AND — BIOLOGY
www.elsevier.com/locate/nucmedbio

Development of ^{68}Ga-labeled mannosylated human serum albumin (MSA) as a lymph node imaging agent for positron emission tomography

Jae Yeon Choi[a,b,c], Jae Min Jeong[a,b,c,*], Byong Chul Yoo[d], Kyunggon Kim[e], Youngsoo Kim[e], Bo Yeun Yang[a,c], Yun-Sang Lee[a,c], Dong Soo Lee[a,c], June-Key Chung[a,b,c], Myung Chul Lee[a]

[a]*Department of Nuclear Medicine, Institute of Radiation Medicine, Seoul National University College of Medicine, Seoul, South Korea*
[b]*Cancer Research Institute, Seoul National University College of Medicine, Seoul, South Korea*
[c]*Department of Radiation Applied Life Sciences, Seoul National University College of Medicine, Seoul, South Korea*
[d]*Research Institute, National Cancer Center, Goyang, Gyeonggi, South Korea*
[e]*Department of Biomedical Sciences, Seoul National University College of Medicine, Seoul, South Korea*

Received 4 August 2010; received in revised form 25 September 2010; accepted 29 September 2010

Abstract

Introduction: Although many sentinel lymph node (SLN) imaging agents labeled with ^{99m}Tc have been developed, no positron-emitting agent has been specifically designed for SLN imaging. Furthermore, the development of the beta probe and the requirement for better image resolution have increased the need for a positron-emitting SLN imaging agent. Here, we describe the development of a novel positron-emitting SLN imaging agent labeled with ^{68}Ga.
Methods: A mannosylated human serum albumin (MSA) was synthesized by conjugating α-D-mannopyranosylphenyl isothiocyanate to human serum albumin in sodium carbonate buffer (pH 9.5), and then 2-(*p*-isothiocyanatobenzyl)-1,4,7-triazacyclononane-1,4,7-triacetic acid was conjugated to synthesize NOTA-MSA. Numbers of mannose and NOTA units conjugated in NOTA-MSA were determined by matrix-assisted laser desorption ionization time-of-flight mass spectrometry. NOTA-MSA was labeled with ^{68}Ga at room temperature. The stability of ^{68}Ga-NOTA-MSA was checked in labeling medium at room temperature and in human serum at 37°C. Biodistribution in normal ICR mice was investigated after tail vein injection, and micro-positron emission tomography (PET) images were obtained after injecting ^{68}Ga-NOTA-MSA into a tail vein or a footpad.
Results: The numbers of conjugated α-D-mannopyranosylphenyl isothiocyanate and 2-(*p*-isothiocyanatobenzyl)-1,4,7-triazacyclononane-1,4,7-triacetic acid units in NOTA-MSA were 10.6 and 6.6, respectively. The labeling efficiency of ^{68}Ga-NOTA-MSA was greater than 99% at room temperature, and its stability was greater than 99% at 4 h. Biodistribution and micro-PET studies of ^{68}Ga-NOTA-MSA showed high liver and spleen uptakes after intravenous injection. ^{68}Ga-NOTA-MSA injected into a footpad rapidly migrated to the lymph node.
Conclusions: ^{68}Ga-NOTA-MSA was successfully developed as a novel SLN imaging agent for PET. NOTA-MSA is easily labeled at high efficiency, and subcutaneously administered ^{68}Ga-NOTA-MSA was found to migrate rapidly to the lymph node.

Keywords: Mannose; Lymphoscintigraphy; NOTA; Ga-68; Gallium; Neomannosyl human serum albumin

1. Introduction

Imaging of the immune system, including the reticuloendothelial system (RES), in the liver, spleen, bone marrow and lymph nodes has been an important field in nuclear medicine. Especially, the imaging of sentinel lymph nodes (SLNs) is important for decision making during breast cancer [1–3] or melanoma [4–6] surgery. Colloidal radiopharmaceuticals labeled with ^{99m}Tc have been used for SLN imaging, and these include ^{99m}Tc-sulfur colloid [7], filtered ^{99m}Tc-sulfur colloid [8], ^{99m}Tc-albumin nanocolloid [9,10], ^{99m}Tc-human serum albumin (HSA) [11], ^{99m}Tc-antimony colloid [12], ^{99m}Tc-phytate [13] and ^{99m}Tc-tin colloid [14]. Particle size is one of the most important characteristics of these agents [15], because particle sizes of <5 nm can penetrate blood capillaries [15] and because ability to access the lymphatic system is reduced as particle size increases. In

* Corresponding author. Department of Nuclear Medicine, Seoul National University Hospital, 101 Daehangno Jongno-gu, Seoul 110-744, South Korea.
E-mail address: jmjng@snu.ac.kr (J.M. Jeong).

0969-8051/$ – see front matter © 2010 Elsevier Inc. All rights reserved.
doi:10.1016/j.nucmedbio.2010.09.010

practice, the ideal particle size of radiocolloids for SLN imaging is slightly larger than 5 nm [15]. The colloids with the smallest particle sizes used for SLN imaging are ^{99m}Tc-antimony trisulfide and ^{99m}Tc-albumin nanocolloid, which have particle sizes between 5 and 50 nm [10,16,17].

Other polymeric agents with smaller particle sizes and mannose residues, such as ^{99m}Tc-diethylene-triaminepentaacetic acid (DTPA)-mannosyl-polylysine [18], ^{99m}Tc-DTPA-mannosyl-dextran [19,20] and ^{99m}Tc-mercaptoacetyl-glycylglycylglycine (MAG_3)-mannosyl-dextran [21], also have been reported to improve SLN imaging. Furthermore, the ^{99m}Tc-DTPA-mannosyl-dextran radiopharmaceutical Lymphoseek entered clinical phase 1 trial [22,23].

A protein molecule HSA with short and long axes of 6 and 8 nm [24], respectively, has adequate size for SLN imaging, and ^{99m}Tc-HSA has thus been used for SLN imaging [11,16]. However, its image has a limitation because it is not recognized by the lymphatic system and does not accumulate in lymph nodes. Accordingly, ^{99m}Tc-mannosylated HSA (MSA) was developed to overcome this problem [17], and MSA was found to be trapped efficiently because macrophages in lymph nodes express mannose receptors on their surfaces [17,25].

The resolution and sensitivity of breast cancer imaging have been greatly improved by positron emission tomography (PET) [26,27]. Furthermore, a beta probe has been developed to detect positrons from lymph node metastases during surgery. This probe has a thin crystal that can detect beta and positron emissions [28]. The superiority of the beta probe for the real-time localization of tumor metastases was recently demonstrated in a comparative study of gamma and beta probes [29]. Generally, [^{18}F]fluorodeoxyglucose has been used for the detection of metastases with a beta probe [30]. However, no specific lymph node-targeting agent labeled with a positron emitter is currently available.

In the present study, we undertook the synthesis of ^{68}Ga-labeled MSA. ^{68}Ga is a known convenient, economical positron emitter [31–33], and MSA was synthesized by conjugating α-D-mannopyranosylphenyl isothiocyanate (SCN-mannose) with HSA. The bifunctional chelating agent 2-(*p*-isothiocyanatobenzyl)-1,4,7-triazacyclononane-1,4,7-triacetic acid (SCN-NOTA) [34] was conjugated to MSA to label MSA with ^{68}Ga (Scheme 1).

2. Materials and methods

2.1. General

HSA and SCN-mannose were purchased from Sigma-Aldrich (St. Louis, MO, USA), and SCN-NOTA was

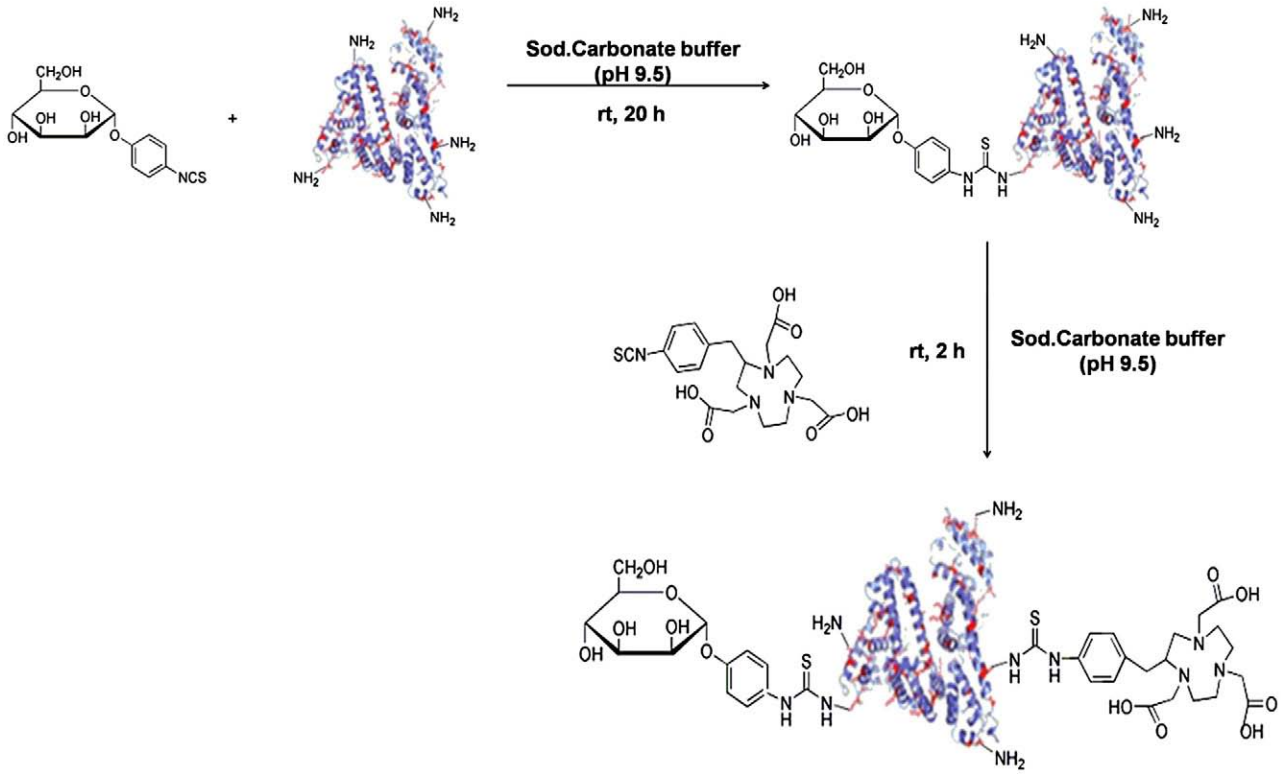

Scheme 1. Two-step synthesis of NOTA-MSA. MSA was synthesized by conjugating SCN-mannose to HSA in sodium carbonate buffer (pH 9.5) at room temperature for 40 h. The reaction mixture was purified using a PD-10 size-exclusion column. NOTA-MSA was prepared by conjugating MSA with (*p*-SCN-Bn)-NOTA in sodium carbonate buffer (pH 9.5) at room temperature for 20 h. The reaction mixture was purified again using a PD-10 column. The molecular weights of the conjugates produced were determined by MALDO-TOF/TOF MS.

purchased from Macrocyclics (Dallas, TX, USA). PD-10 columns (Sephadex G-25 M), which were used for the size-exclusion purification of NOTA-MSA, were purchased from GE Healthcare (Buckinghamshire, UK). Disposable syringe filters (0.2 μm) and instant thin-layer chromatography silica gel (ITLC-SG) plates were purchased from PALL (East Hills, NY, USA). Whatman No. 1 paper was from VWR Scientific (Philadelphia, PA, USA). ^{68}Ge/^{68}Ga generator was purchased from Eckert & Ziegler (Berlin, Germany). Nupage Novex Bis–Tris gradient gel (4%–20%) was purchased from Invitrogen (Carlsbad, CA, USA). Radio-TLC plates were analyzed using a Bio-Scan AR-2000 System imaging scanner (Bio-Scan, Washington, DC, USA). The molecular weights of HSA and its derivatives were determined by matrix-assisted laser desorption ionization time-of-flight/time-of-flight mass spectrometry (MALDI-TOF/TOF MS) using a 4700 Proteomics Analyzer (Applied Biosystems, Foster City, CA, USA). A gamma scintillation counter purchased from Packard Cobra (Meriden, CT, USA) was used for radioactivity measurement, and a micro-PET/CT Rodent R4 microPET scanner (Concorde Microsystems, Knoxville, TN, USA) was used for mouse imaging. The biodistribution study was performed at a laboratory in Seoul National University Hospital, which has full accreditation from the Association for the Assessment and Accreditation of Laboratory Animal Care International (2007). All other reagents and solvents were purchased from Sigma-Aldrich.

2.2. Preparation of NOTA-MSA

HSA (20 mg) was conjugated with SCN-mannose (5.5 mg) in 5 ml of 0.1 M sodium carbonate buffer (pH 9.5) at room temperature for 20 h, as previously described [17]. The reaction mixture was purified using a PD-10 size-exclusion column using 0.1 M sodium carbonate buffer (pH 9.5) as an elution buffer. The purified MSA was stored at −70°C until required for use.

MSA was reacted with SCN-NOTA (10 mg) in 0.1 M sodium carbonate buffer (pH 9.5) for 1 h at room temperature. The resulting NOTA-MSA was purified using a PD-10 size-exclusion column by eluting with a normal saline.

2.3. Mass spectrometric analysis of HSA, MSA and NOTA-MSA

The conjugation numbers of SCN-mannose and SCN-NOTA to HSA were determined by MALDI-TOF/TOF MS. Five microliters of each sample (1 mg/ml of HSA in normal saline, 1 mg/ml of MSA in 0.1 M sodium carbonate buffer, pH 9.5, or 1 mg/ml of NOTA-MSA in normal saline) was mixed with an equal volume of saturated α-cyano-4-hydroxy-cinnamic acid solution in 50% acetonitrile/50% water containing 0.1% TFA. Two microliters of each mixture was then spotted on the target plate and allowed to air-dry prior to mass analysis. Mass spectra were collected in linear mode using an accelerating voltage of 25 kV. The sample spots were ablated with a 337-nm nitrogen laser. Analysis was carried out with 125 scans and 20 laser shots/scan (total of 2500 laser shots). The molecular weights of HSA, MSA and NOTA-MSA were calculated by averaging the results of the 2500 measurements.

2.4. Gel electrophoresis of HSA, MSA and NOTA-MSA

HSA, MSA and NOTA-MSA were subjected to 4%–20% polyacrylamide gel electrophoresis containing 0.1% sodium dodecyl sulfate (SDS-PAGE). Three micrograms of protein was loaded per slot, and gels were stained with Coomassie Brilliant Blue R. The broad-range molecular-weight markers, including myosin (200 kDa), β-galactosidase (116.2 kDa), phosphorylase *b* (97.4 kDa), bovine serum albumin (66.2 kDa), ovalbumin (45 kDa) and carbonic anhydrase (31 kDa), were used as standards.

2.5. Labeling of NOTA-MSA with ^{68}Ga

NOTA-MSA (1 mg in 1 ml of normal saline) was mixed with 1 ml of generator-eluted $^{68}GaCl_3$ (in 0.1 N HCl), and then the pH was adjusted from 1.2 to 9.3 using 0.1 M disodium phosphate and 0.1 M trisodium phosphate. Labeling reactions were performed for 10, 30, 60 and 120 min and at room temperature. Labeling efficiencies and radiochemical purities were determined using ITLC-SG developed with 0.1 M citric acid (R_f values: ^{68}Ga-NOTA-MSA, 0.0; free ^{68}Ga, 1.0) and paper chromatography (for stationary phase, 20–40 μl of 5% bovine serum albumin was spotted on a starting point of Whatman No. 1 paper chromatography strip and dried for 10–15 min at room temperature) developed with normal saline (R_f values: ^{68}Ga-colloid, 0.0; ^{68}Ga-NOTA-MSA, 1.0). ^{68}Ga-colloid was prepared by increasing the pH of $^{68}GaCl_3$ in 0.1 M HCl to 7.5 using 0.1 N $NaHCO_3$ solution.

2.6. Stability testing

The stability of ^{68}Ga-NOTA-MSA was determined in prepared medium (4 h at room temperature) and in human serum (4 h at 37°C). ^{68}Ga-NOTA-MSA and free ^{68}Ga levels were determined using ITLC-SG developed with 0.1 M citric acid as described above.

2.7. Biodistribution study of ^{68}Ga-NOTA-MSA

The biodistribution of ^{68}Ga-NOTA-MSA in ICR mice (male, 20±4 g, n=4) was studied after injecting ^{68}Ga-NOTA-MSA (370 kBq in 0.1 ml of normal saline) via a tail vein. For blocking study, 1 mg of MSA in 0.1 ml of normal saline was injected via a tail vein 10 min before ^{68}Ga-NOTA-MSA injection. Mice were sacrificed at 10 min, 30 min, 1 h and 2 h post-injection. After extracting blood, muscle, heart, lungs, liver, spleen, stomach, intestine, kidneys and femur, we measured the weights and radioactivities of organs using an electronic balance and a gamma scintillation counter, respectively. Results are presented as the percentage of injected dose per gram of tissue (%ID/g).

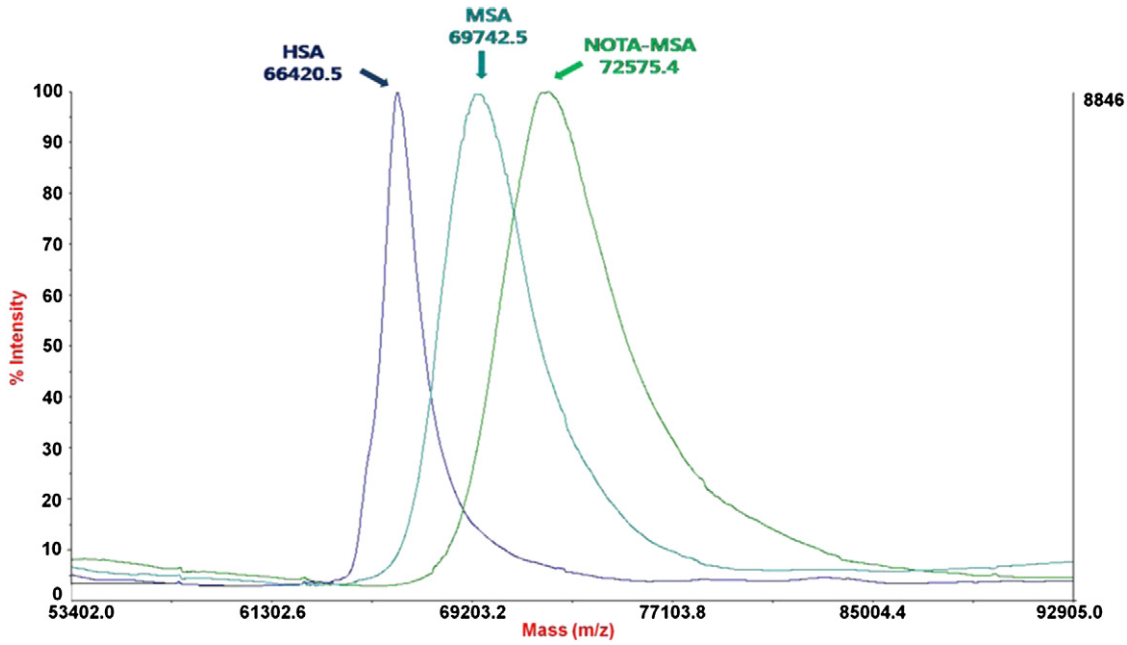

Fig. 1. Linear-mode MALDI-TOF/TOF spectra of HSA, MSA and NOTA-MSA showing the median molecular weights of 66,420, 69,742 and 72,575 Da, respectively. The plot was drawn using Data Explore.

2.8. Micro-PET imaging studies in mice

For intravenous injection imaging, 7.4 MBq of ^{68}Ga-NOTA-MSA in 0.1 ml of normal saline was injected through tail veins of ICR mice and static images were obtained with 10-min acquisitions after 2 h using micro-PET. For subcutaneous injection imaging, dynamic images were obtained for 10 min with 1-min intervals after injection of 0.74 MBq of ^{68}Ga-NOTA-MSA in 0.1 ml into the footpad and analyzed using an IDL version 4.7 software (Research Systems, Boulder, CO, USA). The %ID/g of lymph node was obtained from the images. The cross-calibration factor (CCF) was obtained using a phantom containing 7.4 MBq of ^{68}Ga [CCF=Activity Concentration in Phantom×Branching Ratio/(Value/Pixel)]. Activity concentration C_t at the tissue was calculated from count number (value/pixel) and CCF. Then, %ID/g was obtained from the equation %ID/g=C_t/ID×100%. The pooled image was obtained from the dynamic images and was overlaid on CT image.

3. Results

3.1. The synthesis of NOTA-MSA

The conjugations of SCN-mannose and SCN-NOTA with HSA were performed under weak alkaline condition (pH 9.5): during these reactions, the surface amino groups of albumin conjugate with SCN-mannose and SCN-NOTA. Numbers of SCN-mannose and SCN-NOTA residues conjugated to HSA were determined using MALDI-TOF/TOF MS data (Fig. 1). The spectrum was smoothed due to the mean of 125 measurements with a total of 2500 laser shots. The mean molecular weights of HSA, MSA and NOTA-MSA thus obtained were 66,420±223, 69,742±292 and 72,575±303 Da, respectively. The average numbers of conjugated SCN-mannose and SCN-NOTA residues calculated based on the molecular weights of SCN-mannose (313.3 Da) and NOTA-NCS (429.51 Da) were 10.6±0.8 and 6.6±0.7, respectively.

The higher molecular weights of MSA and NOTA-MSA as compared with HSA were also observed by SDS-PAGE (Fig. 2). The normal shapes of the MSA and NOTA-MSA bands similar to the HSA band represent homogenous distribution of SCN-mannose and SCN-NOTA conjugation.

3.2. Labeling NOTA-MSA with ^{68}Ga

The labeling efficiency of NOTA-MSA with ^{68}Ga was determined using ITLC-SG developed with 0.1 M citric acid

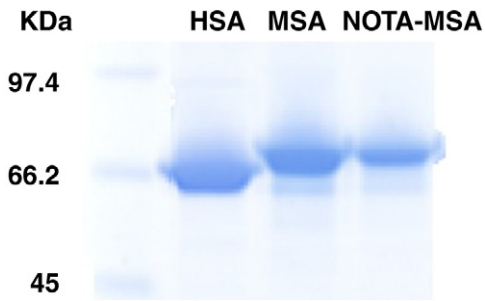

Fig. 2. SDS-PAGE analysis of HSA, MSA and NOTA-MSA using 4%–20% polyacrylamide gel. As the residues are conjugated, the shorter migration distances are demonstrated due to the molecular-weight increase.

and using paper chromatography (bovine serum albumin-impregnated Whatman No. 1 paper) developed with normal saline (Fig. 3). The R_f values of ^{68}Ga-NOTA-MSA and free ^{68}Ga on ITLC-SG were 0.0 and 1.0, respectively (Fig. 3A). In addition, all radioactive components except ^{68}Ga-colloid moved to solvent front on paper chromatography (Fig. 3B). The labeling efficiency of ^{68}Ga-NOTA-MSA was greater than 99% between pH 4.4 and pH 4.8 at room temperature and at 37°C after 30-min incubations. The specific activity of ^{68}Ga-NOTA-MSA was 163 MBq/mg (1.18×10^7 GBq/mol). However, labeling efficiencies were less than 3% at pH 1.0 and pH 8.0 after 120-min incubations (Fig. 4).

Furthermore, the stability of ^{68}Ga-NOTA-MSA was greater than 99% for 4 h both in the prepared medium at room temperature and in human serum at 37°C.

3.3. Biodistribution study of ^{68}Ga-NOTA-MSA

After intravenous injection through a tail vein, ^{68}Ga-NOTA-MSA showed rapid and persistent high liver and spleen uptakes in mice (Table 1), demonstrating the existence of the RES. Femur showed the next highest uptake, indicating the presence of RES in bone marrow. Femoral uptake was lower than that of liver or spleen because the bone marrow portion is low in femur. The

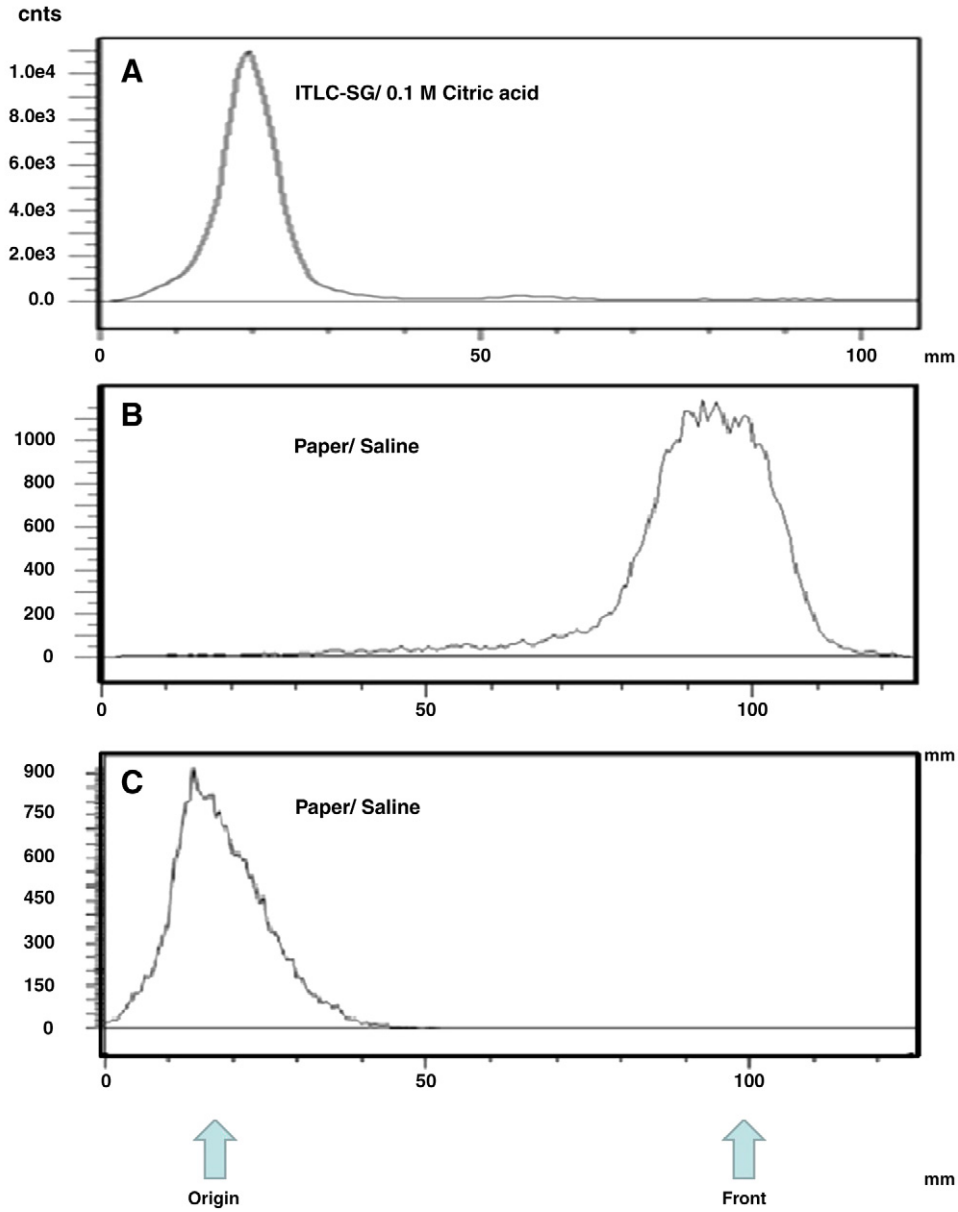

Fig. 3. Radiochemical purity was determined using radio-TLC and paper chromatography. ^{68}Ga-NOTA-MSA remained at the starting point and free ^{68}Ga moved to solvent front on ITLC-SG developed with 0.1 M citric acid (A); ^{68}Ga-NOTA-MSA moved to solvent front (B), while ^{68}Ga-colloid remained at the origin on bovine serum albumin-impregnated Whatman No. 1 paper chromatography developed with normal saline (C).

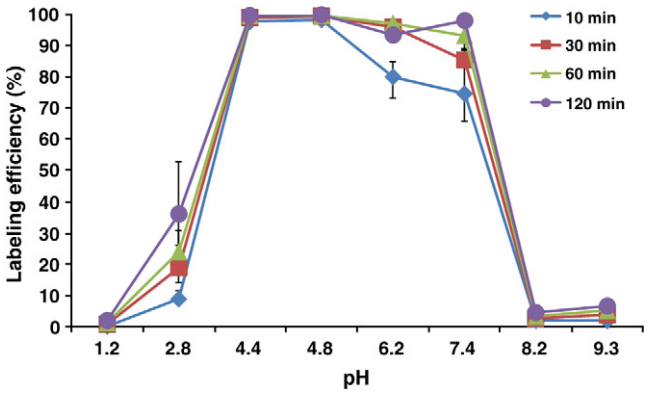

Fig. 4. The relationship between ^{68}Ga labeling efficiency and pH level. NOTA-MSA (1 mg in 1 ml of normal saline) was mixed with 1 ml of $^{68}GaCl_3$ in 0.1 N HCl, and pH was adjusted using 0.1 M disodium phosphate and 0.1 M trisodium phosphate. The mixtures were incubated for 10–120 min at room temperature.

uptakes in liver and spleen were blocked by pre-administration of MSA, which evidenced the existence of mannose receptors. However, most of the other organs, such as muscle, heart, lung, stomach, intestine and kidneys, demonstrated increased uptakes after blocking, because of high blood pool activity due to blocking of RES (Table 1).

3.4. Imaging study in mice

According to our micro-PET study after intravenous injection, ^{68}Ga-NOTA-MSA accumulations in liver, spleen and bone marrow remained almost constant until 2 h post-injection in mice (Fig. 5). Spleen and bone marrow uptakes were only faintly observed due to partial volume effect. Bladder uptake was observed at 2 h.

After subcutaneous injection into left footpads of ICR mice, the inguinal lymph nodes were observed as early as 1 min with persistent activity, which evidences rapid migration of ^{68}Ga-NOTA-MSA into the lymphatic system (Fig. 6A and B). The accurate position of each radioactive site could be seen on the pooled image with an overlaid CT image (Fig. 7).

Table 1
Biodistribution of ^{68}Ga-NOTA-MSA in normal ICR mice after intravenous injection

	10 min (Blocking)	10 min	30 min	1 h	2 h
Blood	38.55±5.96	0.38±0.19	0.13±0.01	0.15±0.02	0.10±0.06
Muscle	1.13±0.04	0.41±0.05	0.32±0.05	0.32±0.10	0.28±0.08
Heart	6.32±1.30	1.39±0.17	1.14±0.28	1.34±0.23	0.89±0.23
Lung	15.53±1.68	2.53±0.17	2.91±0.38	3.22±0.38	2.05±0.38
Liver	20.05±2.52	61.33±3.66	58.85±2.56	61.09±4.77	59.72±5.45
Spleen	10.41±0.30	20.01±2.63	18.64±2.05	20.96±2.54	16.88±0.97
Stomach	0.98±0.03	0.20±0.04	0.25±0.11	0.24±0.03	0.26±0.12
Intestine	1.17±0.06	0.26±0.04	0.28±0.04	0.36±0.02	0.54±0.14
Kidney	8.94±1.59	3.61±0.24	3.26±0.39	3.99±0.17	3.75±0.26
Bone	5.30±0.61	4.44±1.22	4.20±0.45	4.23±0.61	4.35±0.61

Values represent the mean±S.D. %ID/g.

4. Discussion

The feasibility of imaging the lymphatic system using modified polymers or protein to target a specific receptor system has been proven in the nuclear medicine field. The basic goal of receptor targeting using diagnostic agents is to deliver sufficient radioactivity to these receptors. Mannose binding protein, expressed in RES, is an important SLN imaging target of radiolabeled mannosylated agents [35].

In earlier studies, cyanomethyl-2,3,4,6-tetra-*O*-acetyl-1-thio-β-D-mannopyranoside was used to introduce mannosyl residues onto protein molecules, but this process requires several synthetic steps and involves unstable intermediates [36]. In the present study, we used commercially available SCN-mannose to introduce mannose residues and SCN-NOTA to introduce NOTA residues for radiolabeling purpose. The advantage of this method is that the synthetic procedure by formation of thiourea bond is straightforward, and it has thus been used to produce many conjugates [37].

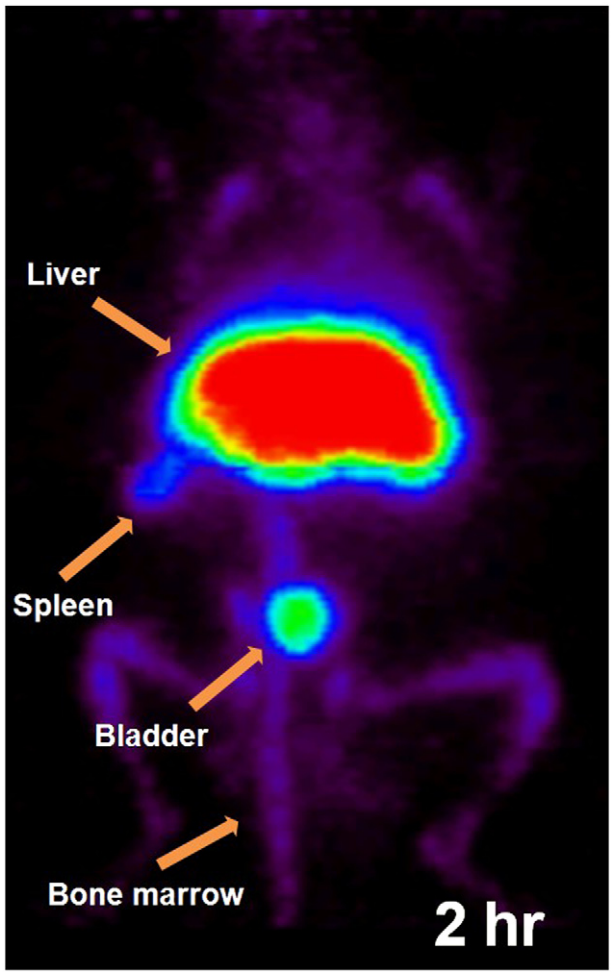

Fig. 5. Micro-PET images of ^{68}Ga-NOTA-MSA in ICR mice after intravenous injection through the tail vein. Images were obtained at 2 h after injection. ^{68}Ga activity is high in liver and faint in spleen and bone marrow. Splenic and bone marrow uptakes appear lower than real uptakes due to the partial volume effect. Furthermore, uptakes remained constant for 2 h.

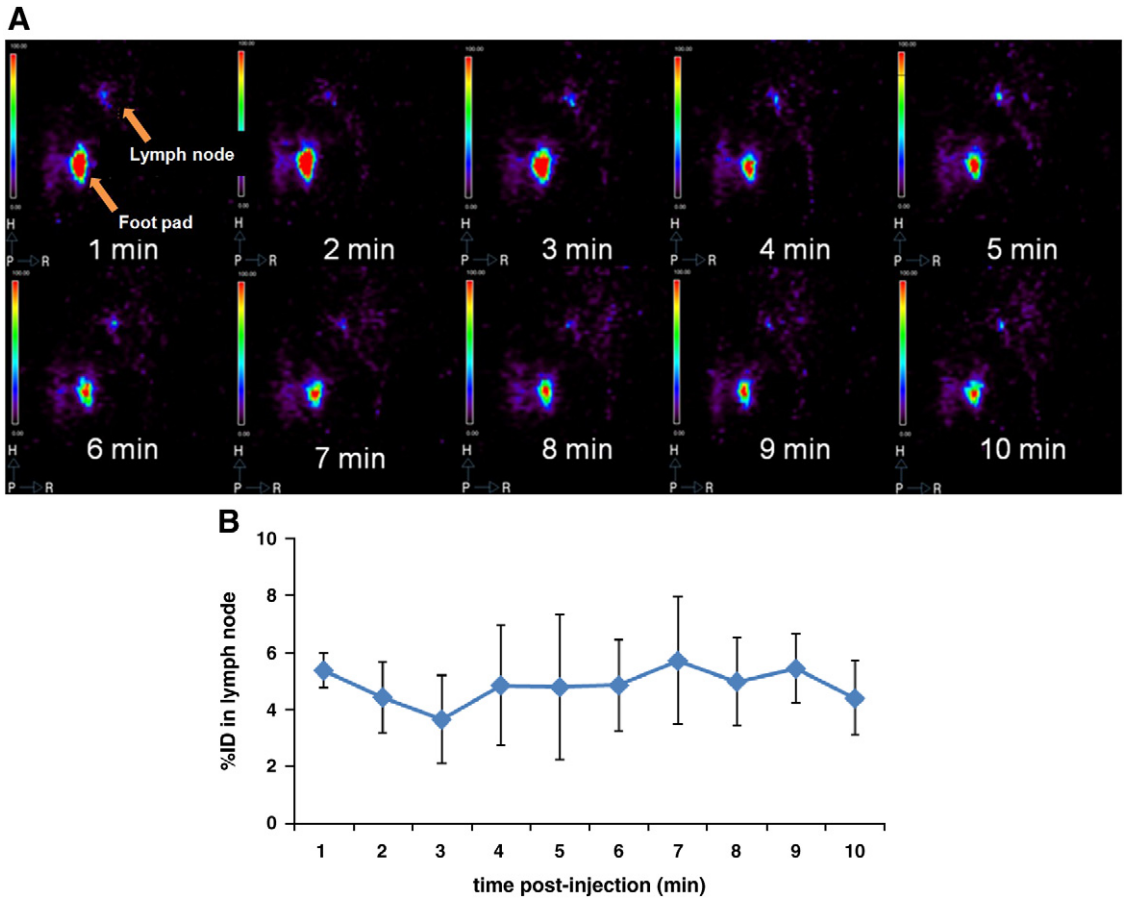

Fig. 6. Micro-PET dynamic images of ^{68}Ga-NOTA-MSA for 10 min after subcutaneous injection at the footpad. Lymph node uptake was seen at 1 min (A), and quantification of the uptake showed almost constant activity in the lymph node (B). Lymph node uptake might be underestimated due to the partial volume effect.

We found that a weakly alkaline sodium carbonate buffer (pH 9.5) provided a suitable environment for thiourea bond formation between isothiocyanate and amino groups.

In the present study, conjugation reactions were performed stepwise, and numbers of SCN-mannose and SCN-NOTA residues conjugated were measured after each step. ^{68}Ga-NOTA-MSA produced was purified by size-exclusion column and analyzed by MALDI-TOF/TOF MS, which showed that 9.2 and 6.5 residues of SCN-mannose and SCN-NOTA, respectively, were conjugated. The reproducibility of MALDI-TOF MS for determining numbers of bound ligands has been previously described [38]. In addition, SDS-PAGE was used to confirm molecular-weight increase due to HSA derivatization.

^{68}Ga labeling on NOTA-MSA was performed effectively at room temperature and pH 4.4–6.2. Furthermore, high labeling yields were obtained even at room temperature because NOTA was used as a bifunctional chelating agent. It has been reported that the NOTA–Ga(III) complexes are extremely stable due to the dimensional match between the NOTA complexing site and the ionic radius of Ga(III) [39–41]. Had we used the more popular compound DOTA as a bifunctional chelating agent, heating may have been required to achieve labeling, and this might have detrimental effects on heat-labile proteins such as HSA. The thermodynamic stability constants (log K) of Ga(III)–DOTA [42] and Ga(III)–NOTA [43] complexes have been reported to be

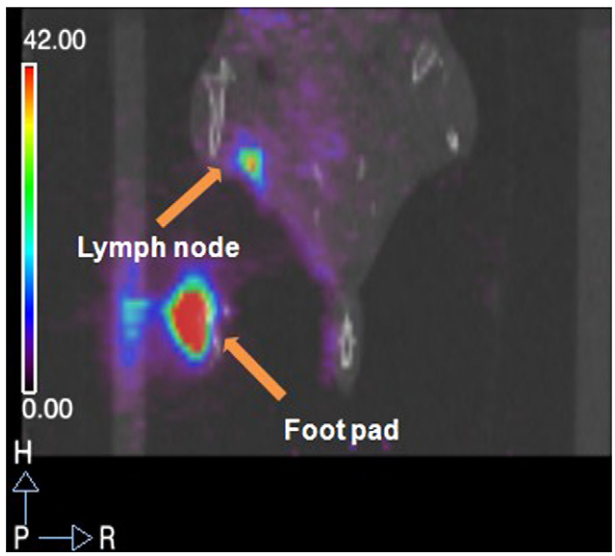

Fig. 7. Pooled micro-PET/CT image of ^{68}Ga-NOTA-MSA for 10 min after subcutaneous injection at the footpad. The PET image is overlaid on the CT image.

21.33 and 30.98, respectively. We also found that ^{68}Ga-NOTA-MSA was stable for at least 4 h in prepared medium at room temperature and in human serum at 37°C. The stability in human serum at 37°C partially represents the in vivo stability.

^{68}Ga (89% β^+ emission, $t_{1/2}$=67.6 min) is an emerging radioisotope for PET due to its availability from the straightforward and economical ^{68}Ge/^{68}Ga generator [32,33] and the ease with which radiolabeling is accomplished. Generally, radiolabeled high molecular-weight protein agents require a long washout time from non-target tissues for PET imaging, and ^{18}F is thus commonly used as a label because of its relatively long half-life (110 min) [44]. However, SLN imaging can be performed in less than 1 h post-injection, which means that ^{68}Ga has a suitable half-life. Furthermore, ^{18}F-labeling requires considerable preparation time prior to injection — that is, cyclotron operation, the evaporation of water and solvent and radiolabeling, which all take at least 1–2 h. However, ^{68}Ga labeling requires only 20 min of preparation time for generator elution and radiolabeling steps. In addition, ^{68}Ga labeling kits could be formulated to simplify the labeling procedure further [45].

Furthermore, the high positron energy ($E\beta_{+max}$=1.9 MeV) of ^{68}Ga provides deeper tissue penetration and better detection yields when the beta probe is used, which are both advantageous for SLN detection. In fact, [^{18}F] fluorodeoxyglucose ($E\beta_{+max}$=0.69 MeV), which is currently used for SLN detection in combination with beta probe, has a maximum range in tissue of only 2.4 mm, whereas that of ^{68}Ga is 9.2 mm. This topic of tissue penetration is of considerable importance because most lymph nodes are buried in tissue, and tissue penetration distance is critical when the beta probe is used to detect lymph nodes during surgery.

When ^{68}Ga-NOTA-MSA was injected through a tail vein, we found the highest distributions in the liver, followed by the spleen (Table 1). The relatively higher uptake in the femur than the other tissues is due to the existence of bone marrow inside it. These findings demonstrate that ^{68}Ga-NOTA-MSA was specifically taken up by RES. The blocking study after pre-injection of MSA demonstrated decreased uptakes in liver and spleen, which represent the specific uptake by mannose receptor (Table 1). Blood uptake was very high after blocking, which is also attributed to high uptakes in other tissues, such as muscle, heart, lung, stomach, intestine and kidneys (Table 1). The micro-PET images obtained also showed persistent uptakes in liver, spleen and bone marrow after intravenous injection (Fig. 5). Although uptakes by spleen and bone marrow were lower than that by liver in our biodistribution study, micro-PET imaging showed even lower uptakes by spleen and bone marrow because of the partial volume effect. Bladder activity demonstrates the excretion of metabolites through the kidney. On the other hand, when ^{68}Ga-NOTA-MSA was administered subcutaneously into footpads, it was found by dynamic micro-PET imaging to rapidly migrate to the inguinal region, which is regarded to indicate lymph node uptake and shows the feasibility of using this agent for SLN imaging and detection. These data are consistent with previous reports (Fig. 6A and B) [17,46].

The majority of the currently available SLN imaging and detection agents are labeled with gamma emitters, such as ^{99m}Tc, which can be imaged using a planar gamma camera or by single photon emission computed tomography. Although ^{99m}Tc is the most readily available radionuclide in practical nuclear medicine, gamma ray imaging instruments are intrinsically limited in terms of counting efficiency and image resolution, because collimators, which basically restrict gamma ray flow to the detector, should be used. Furthermore, the worldwide instability of ^{99}Mo supply requires that new agents labeled with radionuclides other than ^{99m}Tc be developed. Thus, the development of positron-emitting SLN imaging agents would make an important progress in this field.

5. Conclusions

In the present study, we developed ^{68}Ga-NOTA-MSA for immune system imaging. ^{68}Ga-NOTA-MSA can be imaged and detected by PET and a beta probe, respectively. The novel NOTA-MSA precursor was synthesized and labeled with generator-eluted ^{68}Ga at room temperature with high efficiency (>99%). Furthermore, the ^{68}Ga-NOTA-MSA produced was stable, showed high uptakes in RES-containing tissues, such as liver, spleen and femur, after intravenous injection into mice and rapidly migrated to lymph nodes after being subcutaneously injected into mice footpads. The development of ^{68}Ga-NOTA-MSA will hopefully encourage the development of other positron-emitting agents for immune system imaging and SLN detection.

Acknowledgments

This work was supported by NRF of Korea through Grants R0A-2008–000-20116-0 and 2010K001055, funded by the Ministry of Education, Science and Technology.

References

[1] Mariani G, Moresco L, Viale G, Villa G, Bagnasco M, Canavese G, et al. Radioguided sentinel lymph node biopsy in breast cancer surgery. J Nucl Med 2001;42:1198–215.

[2] Mirzaei S, Rodrigues M, Hoffmann B, Knoll P, Riegler-Keil M, Kreuzer W, et al. Sentinel lymph node detection with large human serum albumin colloid particles in breast cancer. Eur J Nucl Med Mol Imaging 2003;30:874–8.

[3] Pain SJ, Barber RW, Ballinger JR, Solanki CK, O'Mahony S, Mortimer PS, et al. Side-to-side symmetry of radioprotein transfer from tissue space to systemic vasculature following subcutaneous injection in normal subjects and patients with breast cancer. Eur J Nucl Med Mol Imaging 2003;30:657–61.

[4] Mariani G, Gipponi M, Moresco L, Villa G, Bartolomei M, Mazzarol G, et al. Radioguided sentinel lymph node biopsy in malignant cutaneous melanoma. J Nucl Med 2002;43:811–27.

[5] Uren RF, Howman-Giles R, Thompson JF. Patterns of lymphatic drainage from the skin in patients with melanoma. J Nucl Med 2003;44:570–82.
[6] Bartolomei M, Testori A, Chinol M, Gennari R, De Cicco C, Leonardi L, et al. Sentinel node localization in cutaneous melanoma: lymphoscintigraphy with colloids and antibody fragments versus blue dye mapping. Eur J Nucl Med 1998;25:1489–94.
[7] Stern HS, McAfee JG, Subramanian G. Preparation, distribution and utilization of technetium-99m-sulfur colloid. J Nucl Med 1966;7: 665–75.
[8] Hung JC, Wiseman GA, Wahner HW, Mullan BP, Taggart TR, Dunn WL. Filtered technetium-99m-sulfur colloid evaluated for lymphoscintigraphy. J Nucl Med 1995;36:1895–901.
[9] McAfee JG, Subramanian G, Aburano T, Thomas FD, Fernandes P, Gagne G, et al. A new formulation of Tc-99m minimicroaggregated albumin for marrow imaging: comparison with other colloids, In-111 and Fe-59. J Nucl Med 1982;23:21–8.
[10] Leidenius MH, Leppanen EA, Krogerus LA, Smitten KA. The impact of radiopharmaceutical particle size on the visualization and identification of sentinel nodes in breast cancer. Nucl Med Commun 2004;25:233–8.
[11] Yang SS, Nickoloff EL, McIntyre PA, Maddrey WC, Mikesell HH, Scheffel U, et al. Tc-99m human serum albumin: a suitable agent for plasma volume measurements in man. J Nucl Med 1978;19:804–7.
[12] Martindale AA, Papadimitriou JM, Turner JH. Technetium-99m antimony colloid for bone-marrow imaging. J Nucl Med 1980;21: 1035–41.
[13] Seok JW, Kim IJ. Comparison of the efficiency for Tc-99m tin-colloid and Tc-99m phytate in sentinel node detection in breast cancer patients. Nucl Med Mol Imaging 2008;42:451–5.
[14] Seok JW, Jun S, Nam HY, Kim IJ. Comparison between the 1 day and the 2 day protocols of lymphoscintigraphy and sentinel node biopsy using subareolar injection in breast cancer patients: a retrospective study. Nucl Med Mol Imaging 2009;43:55–9.
[15] Jeong JM, Hong MK, Kim YJ, Lee J, Kang JH, Lee DS, et al. Development of ^{99m}Tc-neomannosyl human serum albumin (^{99m}Tc-MSA) as a novel receptor binding agent for sentinel lymph node imaging. Nucl Med Commun 2004;25:1211–7.
[16] Henze E, Schelbert HR, Collins JD, Najafi A, Barrio JR, Bennett LR. Lymphoscintigraphy with Tc-99m-labeled dextran. J Nucl Med 1982;23:923–9.
[17] Jang SJ, Moon SH, Kim SK, Kim BS, Kim SW, Chung KW, Lee ES, et al. Comparison of the results for sentinel lymph node mapping in the breast cancer patients using ^{99m}Tc-antimony trisulfide colloid, ^{99m}Tc-tin colloid, and ^{99m}Tc-human serum albumin. Nucl Med Mol Imaging 2007;41:546–52.
[18] Vera DR, Wisner ER, Stadalnik RC. Sentinel node imaging via a nonparticulate receptor-binding radiotracer. J Nucl Med 1997;38:530–5.
[19] Vera DR, Wallace AM, Hoh CK, Mattrey RF. A synthetic macromolecule for sentinel node detection: ^{99m}Tc-DTPA-mannosyl-dextran. J Nucl Med 2001;42:951–9.
[20] Hoh CK, Wallace AM, Vera DR. Preclinical studies of [^{99m}Tc]DTPA-mannosyl-dextran. Nucl Med Biol 2003;30:457–64.
[21] Vera DR, Wallace AM, Hoh CK. [^{99m}Tc]MAG_3-mannosyl-dextran: a receptor-binding radiopharmaceutical for sentinel node detection. Nucl Med Biol 2001;28:493–8.
[22] Wallace AM, Hoh CK, Vera DR, Darrah DD, Schulteis G. Lymphoseek: a molecular radiopharmaceutical for sentinel node detection. Ann Surg Oncol 2003;10:531–8.
[23] Wallace AM, Hoh CK, Ellner SJ, Darrah DD, Schulteis G, Vera DR. Lymphoseek: a molecular imaging agent for melanoma sentinel lymph node mapping. Ann Surg Oncol 2007;14:913–21.
[24] He XM, Carter DC. Atomic structure and chemistry of human serum albumin. Nature 1992;358:209–15.
[25] Kim S, Jeong JM, Hong MK, Jang JJ, Lee J, Lee DS, et al. Differential receptor targeting of liver cells using ^{99m}Tc-neoglycosylated human serum albumins. Arch Pharm Res 2008;31:60–6.
[26] Mankoff DA, Eubank WB. Current and future use of positron emission tomography (PET) in breast cancer. J Mammary Gland Biol Neoplasia 2006;11:125–36.
[27] Cho YS, Choi JY, Lee SJ, Hyun SH, Lee JY, Choi Y, Choe YS, et al. Clinical significance of focal breast lesions incidentally identified by ^{18}F-FDG PET/CT. Nucl Med Mol Imaging 2008;42:456–63.
[28] Daghighian F, Mazziotta JC, Hoffman EJ, Shenderov P, Eshaghian B, Siegel S, et al. Intraoperative beta probe: a device for detecting tissue labeled with positron or electron emitting isotopes during surgery. Med Phys 1994;21:153–7.
[29] Strong VE, Galanis CJ, Riedl CC, Longo VA, Daghighian F, Humm JL, et al. Portable PET probes are a novel tool for intraoperative localization of tumor deposits. Ann Surg Innov Res 2009;3:2.
[30] Essner R, Hsueh EC, Haigh PI, Glass EC, Huynh Y, Daghighian F. Application of an [^{18}F]fluorodeoxyglucose-sensitive probe for the intraoperative detection of malignancy. J Surg Res 2001;96:120–6.
[31] Ehrhardt GJ, Welch MJ. A new germanium-63/gallium-68 generator. J Nucl Med 1978;19:925–9.
[32] Ambe S. Ge-68–Ga-68 generator with alpha-ferric oxide support. Appl Radiat Isot 1988;39:49–51.
[33] Zhernosekov KP, Filosofov DV, Baum RP, Aschoff P, Bihl H, Razbash AA, et al. Processing of generator-produced Ga-68 for medical application. J Nucl Med 2007;48:1741–8.
[34] Studer M, Meares CF. Synthesis of novel 1,4,7-triazacyclononane-*N*,*N*′,*N*″-triacetic acid derivatives suitable for protein labeling. Bioconjug Chem 1992;3:337–41.
[35] Mendez J, Wallace AM, Hoh CK, Vera DR. Detection of gastric and colonic sentinel nodes through endoscopic administration of ^{99m}Tc-DTPA-mannosyl-dextran in pigs. J Nucl Med 2003;44:1677–81.
[36] Chipowsky S, Yuan CL. Synthesis of 1-thioaldosides having an amino group at the aglycon terminal. Carbohydrate Res 1973;31:339–46.
[37] Jeong JM, Hong MK, Chang YS, Lee YS, Kim YJ, Cheon GJ, et al. Preparation of a promising angiogenesis PET imaging agent: ^{68}Ga-labeled c(RGDyK)-isothiocyanatobenzyl-1,4,7-triazacyclononane-1,4,7-triacetic acid and feasibility studies in mice. J Nucl Med 2008; 49:830–6.
[38] Di Stefano G, Tubaro M, Lanza M, Boga C, Fiume L, Traldi P. Synthesis and physicochemical characteristics of a liver-targeted conjugate of fluorodeoxyuridine monophosphate with lactosaminated human albumin. Rapid Commun Mass Spectrom 2003;17:2503–7.
[39] Parker D. Tumor targeting with radiolabeled macrocycle antibody conjugates. Chem Soc Rev 1990;19:271–91.
[40] Lee J, Garmestani K, Wu C, Brechbiel MW, Chang HK, Choi CW, et al. In vitro and in vivo evaluation of structure–stability relationship of ^{111}In- and ^{67}Ga-labeled antibody via 1B4M or C-NOTA chelates. Nucl Med Biol 1997;24:225–30.
[41] Jeong JM, Kim YJ, Lee YS, Lee DS, Chung JK, Lee MC. Radiolabeling of NOTA and DOTA with positron emitting ^{68}Ga and investigation of in vitro properties. Nucl Med Mol Imaging 2009;43: 330–6.
[42] Clarke ET, Martell AE. Stabilities of trivalent metal–ion complexes of the tetraacetate derivatives of 12-membered, 13-membered and 14-membered tetraazamacrocycles. Inorg Chim Acta 1991;190:37–46.
[43] Clarke ET, Martell AE. Stabilities of the Fe(Iii), Ga(Iii) and in(Iii) chelates of *N*,*N*′,*N*″-triazacyclononanetriacetic acid. Inorg Chim Acta 1991;181:273–80.
[44] Chang YS, Jeong JM, Lee YS, Kim HW, Rai GB, Lee SJ, et al. Preparation of ^{18}F-human serum albumin: a simple and efficient protein labeling method with ^{18}F using a hydrazone-formation method. Bioconjug Chem 2005;16:1329–33.
[45] Yang BY, Jeong JM, Kim YJ, Choi JY, Lee YS, Lee DS, et al. Formulation of ^{68}Ga BAPEN kit for myocardial positron emission tomography imaging and biodistribution study. Nucl Med Biol 2010;37:149–55.
[46] Takagi K, Uehara T, Kaneko E, Nakayama M, Koizumi M, Endo K, et al. ^{99m}Tc-labeled mannosyl-neoglycoalbumin for sentinel lymph node identification. Nucl Med Biol 2004;31:893–900.